Physics Letters B 767 (2017) 437–442

Contents lists available at ScienceDirect

Physics Letters B

www.elsevier.com/locate/physletb

Theoretical study on production of heavy neutron-rich isotopes around the $N = 126$ shell closure in radioactive beam induced transfer reactions

Long Zhu [a,*], Jun Su [a], Wen-Jie Xie [b,c], Feng-Shou Zhang [d,e,f]

[a] Sino-French Institute of Nuclear Engineering and Technology, Sun Yat-sen University, Zhuhai 519082, China
[b] Department of Physics, Yuncheng University, Yuncheng 044000, China
[c] Institute of Modern Physics, Chinese Academy of Sciences, Lanzhou 730000, China
[d] The Key Laboratory of Beam Technology and Material Modification of Ministry of Education, College of Nuclear Science and Technology, Beijing Normal University, Beijing 100875, China
[e] Beijing Radiation Center, Beijing 100875, China
[f] Center of Theoretical Nuclear Physics, National Laboratory of Heavy Ion Accelerator of Lanzhou, Lanzhou 730000, China

ARTICLE INFO

Article history:
Received 19 November 2016
Received in revised form 23 December 2016
Accepted 21 January 2017
Available online 20 February 2017
Editor: W. Haxton

ABSTRACT

In order to produce more unknown neutron-rich nuclei around $N = 126$, the transfer reactions ^{136}Xe + ^{198}Pt, $^{136-144}$Xe + ^{208}Pb, and ^{132}Sn + ^{208}Pb are investigated within the framework of the dinuclear system (DNS) model. The influence of neutron excess of projectile on production cross sections of target-like products is studied through the reactions ^{136,144}Xe + ^{208}Pb. We find that the radioactive projectile ^{144}Xe with much larger neutron excess is favorable to produce neutron-rich nuclei with charge number less than the target rather than produce transtarget nuclei. The incident energy dependence of yield distributions of fragments in the reaction ^{132}Sn + ^{208}Pb are also studied. The production cross sections of neutron-rich nuclei with $Z = 72$–77 are predicted in the reactions $^{136-144}$Xe + ^{208}Pb and ^{132}Sn + ^{208}Pb. It is noticed that the production cross sections of unknown neutron-rich nuclei in the reaction ^{144}Xe + ^{208}Pb are at least two orders of magnitude larger than those in the reaction ^{136}Xe + ^{208}Pb. The radioactive beam induced transfer reactions ^{139,144}Xe + ^{208}Pb, considering beam intensities proposed in SPIRAL2 (Production System of Radioactive Ion and Acceleration On-Line) project as well, for production of neutron-rich nuclei around the $N = 126$ shell closure are investigated for the first time. It is found that, in comparison to the stable beam ^{136}Xe, the radioactive beam ^{144}Xe shows great advantages for producing neutron-rich nuclei with $N = 126$ and the advantages get more obvious for producing nuclei with less charge number.

1. Introduction

The multinucleon transfer process in collisions of heavy ions, which is one promising way to produce heavy nuclei on neutron-rich side of the stability line, has been investigated in many works. Thirty years ago, there had been a great interest in use of the transfer reactions with actinide targets to produce new transtarget nuclei [1–6]. Fm and Md neutron-rich isotopes have been produced at the level of 0.1 μb. Recently, a lot of experiments has been performed to investigate the multinucleon transfer reactions [7–14]. To better understand mechanism of heavy elements synthesis in the *r*-process, the production of neutron-rich nuclei along $N = 126$ has also been studied [12–16]. Based on the structural properties [17], the reaction ^{136}Xe + ^{208}Pb is proposed to produce unknown neutron-rich isotopes in the region of the neutron shell closure $N = 126$ [16]. However, new isotopes were not observed [12,13]. The production of neutron-rich nuclei with $N = 126$ through multinucleon transfer reaction ^{136}Xe + ^{198}Pt were reported by Watanabe et al. [14]. The huge advantages of using multinucleon transfer process for the production of very neutron-rich nuclei with $N = 126$ were noticed and the advantages became more and more striking when the atomic number was lower. In Ref. [14], the authors also found that due to small number of evaporated neutrons, the production of the very neutron-rich nuclei were mainly through collisions involving a small kinetic energy loss.

* Corresponding author.
E-mail address: zhulong@mail.sysu.edu.cn (L. Zhu).

http://dx.doi.org/10.1016/j.physletb.2017.01.082

The mechanisms of deep inelastic collisions were studied by Zagrebaev and Greiner in many works [15,16,18,19]. It is found that shell effects may significantly enhance the yield of neutron-rich heavy nuclei for appropriate projectile-target combinations [18] and optimal beam energy for production of neutron-rich nuclei in transfer reactions is about 20–30 MeV higher than the corresponding Coulomb barrier in the entrance channel [19]. To understand the dynamical process of the deep inelastic collisions, some microscopical dynamics models, such as the time-dependent Hartree–Fock (TDHF) [20–24] and quantum molecular dynamics (QMD) model [25–27] are developed. The semiclassical model GRAZING describes quite well the collisions with large impact parameters [28]. The dinuclear system (DNS) model, which can treat the charge, mass, angular momentum, and kinetic energy dissipation during heavy ion collisions, has been successfully used in investigating the multinucleon transfer reactions [29–34].

It is noticed that the transfer reactions with stable combinations can only produce moderately neutron-rich nuclei with reachable cross sections [29]. Nowadays, with the development of the modern radioactive beam facilities such as the proposed SPIRAL2 (Production System of Radioactive Ion and Acceleration On-Line) facility at GANIL (Grand Accélérateur National dIons Lourds) [35], the high intensities of neutron-rich beams can be provided. Due to larger neutron excess of radioactive beams, larger cross sections are expected for production of neutron-rich isotopes far from the stability line. Because of the problems with producing, separating and detecting the transfer reaction products, the heavy neutron-rich region with mass $A > 170$ has not been studied yet, especially the structural properties of neutron-rich nuclei along the neutron shell $N = 126$. Therefore, it is necessary to investigate radioactive beam induced transfer reactions for the choice of optimal projectile-target combinations, although the intensities of the radioactive beams are smaller than those of stable ones.

In this work, the transfer reactions ^{136}Xe + ^{198}Pt, $^{136-144}$Xe + ^{208}Pb, and ^{132}Sn + ^{208}Pb are investigated within the framework of DNS model. We investigate how the production cross sections of target-like fragments (TLFs) evolve as the projectile acquires a larger neutron excess. The evolution of yield distributions of fragments as a function of their N/Z ratios with the increasing incident energy are also investigated. The production cross sections of neutron-rich isotopes with $N = 126$ in the radioactive induced transfer reactions ^{139,144}Xe + ^{208}Pb and ^{132}Sn + ^{208}Pb are predicted. According to the intensities of radioactive beams proposed in Ref. [35], the prospects for production of neutron-rich isotopes with $N = 126$ in radioactive beam induced transfer reactions are evaluated quantitatively.

The article is organized as follows. In Sec. 2, we describe the DNS model. The results and discussion are presented in Sec. 3. Finally, we summarize the main results in Sec. 4.

2. Model

The DNS model assumes a sudden potential energy surface in the radial coordinate, and adiabatic behavior in the mass asymmetry coordinate. Actually, in multinucleon transfer reactions, especially for the reactions with no potential pockets, the dynamical process in the radial coordinate is weak and the evolution of DNS is mainly in mass asymmetry degree.

In DNS model, the distribution probability $P(Z_1, N_1, t)$ for fragment 1 with proton number Z_1 and neutron number N_1 at time t can be calculated by solving the following master equation:

$$\begin{aligned}\frac{dP(Z_1,N_1,t)}{dt} &= \sum_{Z_1'} W_{Z_1,N_1;Z_1',N_1}(t)[d_{Z_1,N_1}P(Z_1',N_1,t) \\ &\quad - d_{Z_1',N_1}P(Z_1,N_1,t)] \\ &\quad + \sum_{N_1'} W_{Z_1,N_1;Z_1,N_1'}(t)[d_{Z_1,N_1}P(Z_1,N_1',t) \\ &\quad - d_{Z_1,N_1'}P(Z_1,N_1,t)] \\ &\quad - [\Lambda_{\rm qf}(\Theta(t)) + \Lambda_{\rm fis}(\Theta(t))]P(Z_1,N_1,t). \end{aligned} \quad (1)$$

Here $W_{Z_1,N_1;Z_1',N_1}$ ($W_{Z_1,N_1;Z_1,N_1'}$) denotes the mean transition probability from the channel (Z_1, N_1) to (Z_1', N_1) [or (Z_1, N_1) to (Z_1, N_1')], and d_{Z_1,N_1} is the microscopic dimension corresponding to the macroscopic state (Z_1, N_1). In the DNS model, we consider the process of only one nucleon transfer. The sum is taken over all possible proton and neutron numbers that fragment 1 may take. $\Lambda_{\rm qf}$ is the quasifission rate, which describes the evolution of DNS system along relative distance R. $\Lambda_{\rm fis}$ describes the fission probability of heavy fragment in DNS. The detailed description of $\Lambda_{\rm qf}$ and $\Lambda_{\rm fis}$ can be seen in Ref. [36].

The potential energy surface (PES) can be written as

$$\begin{aligned}U(Z_1,N_1,R_{\rm cont}) &= B(Z_1,N_1) + B(Z_2,N_2) \\ &\quad + V_{\rm CN}(Z_1,N_1,R_{\rm cont}), \end{aligned} \quad (2)$$

where, $B(Z_i, N_i)$ ($i = 1, 2$) is the ground state binding energy of the fragment i. The effective nucleus–nucleus interaction potential $V_{\rm CN}(Z_1, N_1, R_{\rm cont})$ can be written as

$$V_{\rm CN}(Z_1,N_1,R_{\rm cont}) = V_{\rm N}(Z_1,N_1,R_{\rm cont}) + V_{\rm C}(Z_1,N_1,R_{\rm cont}). \quad (3)$$

For the reactions with no potential pockets, the position where the nucleon transfer process takes place can be get with the equation: $R_{\rm cont} = R_1(1+\beta_1 Y_{20}(\theta_1)) + R_2(1+\beta_2 Y_{20}(\theta_2)) + 0.7$ fm. Here, $R_{1,2} = 1.16A_{1,2}^{1/3}$. $\beta_{1,2}$ is the quadrupole deformation parameter of the fragments and is taken from Ref. [37]. $\theta_i = 0$ for tip-tip collisions. The detailed description of nuclear potential $V_{\rm N}$ and Coulomb potential $V_{\rm C}$ can be seen in Ref. [38]. The diffuseness parameter is $a = 0.6$ fm in this work.

The production cross sections of the primary products in transfer reactions can be calculated as follows:

$$\begin{aligned}\sigma_{\rm pr}(Z_1,N_1) &= \frac{\pi\hbar^2}{2\mu E_{\rm c.m.}} \sum_{J=0}^{J_{\rm max}} (2J+1)T_{\rm cap} \\ &\quad \times P(Z_1,N_1,t=\tau_{\rm int}), \end{aligned} \quad (4)$$

where, $T_{\rm cap}$ is the capture probability. Because there are no potential pockets for multinucleon transfer reactions in this work and the incident energies are above the interaction potentials at the contact configurations (there are no ordinary barriers: the potential energies of these nuclei are everywhere repulsive), it is reasonable to take the value of $T_{\rm cap}$ as 1. The interaction time $\tau_{\rm int}$, which is determined by deflection function method [39], is strongly affected by interaction potential at the contact configuration, incident energy, and entrance angular momentum J.

The excitation energy of the DNS can be written as

$$E^*_{\rm DNS}(Z_1,N_1) = E_{\rm diss} - [U(Z_1,N_1,R_{\rm cont}) - U(Z_{\rm p},N_{\rm p},R_{\rm cont})]. \quad (5)$$

Here, $E_{\rm diss}$ is the energy dissipated into the composite system from the incident energy, which depends on entrance angular momentum J. The subscript "p" denotes initial configuration of DNS. Assuming the situation of thermal equilibrium, the sharing of the

excitation energy between primary fragments is assumed to be proportional to their masses.

The code GEMINI is used to treat the sequential statistical evaporation of excited fragments. Subsequent de-excitation cascades of the excited fragments via emission of light particles (neutron, proton, and α) and gamma-rays competing with the fission process are taken into account, which lead to the final mass distribution of the reaction products.

3. Results and discussion

In Fig. 1, the calculated production cross sections of projectile-like fragments (PLFs) in the reaction ^{136}Xe + ^{198}Pt are compared with the recent experimental data [14]. The incident energy $E_{\rm c.m.} = 643$ MeV. For this system, the interaction potential at the contact point $V_{\rm CN} = 340$ MeV. The dashed lines denote the distributions of primary fragments. It can be seen that almost 6 neutrons are evaporated in de-excitation process. It is noticed that as more protons are stripped (picked up), the mass number at the peak drifts to lower (higher) A, which is the same trend as the experimental data shows. Also, one can see that for proton pick up channels the mass numbers of peak positions are in a good agreement with the experimental data.

The study of the evolution of production cross sections of TLFs as the projectile acquires a larger neutron excess is necessary for the choice of transfer reactions. We show the calculated production cross sections of TLFs in the reactions ^{136}Xe + ^{208}Pb and ^{144}Xe + ^{208}Pb in Fig. 2. The calculated cross sections for producing various TLFs in transfer reactions ^{136}Xe + ^{208}Pb are compared with experimental data [13] at $E_{\rm c.m.} = 450$ MeV $= 1.06 \times V_{\rm CN}$. In order to take comparison with the radioactive beam induced reaction ^{144}Xe + ^{208}Pb, the incident energy for this reaction is also taken as $1.06 \times V_{\rm CN}$. The $V_{\rm CN}$ for the reactions ^{136}Xe + ^{208}Pb and ^{144}Xe + ^{208}Pb are 423 and 406 MeV, respectively. It is shown that our calculations underestimate the experimental cross sections for the production of transtarget nuclei [see Figs. 2(e)–2(h)]. Much better descriptions can be seen for the proton pick up from ^{208}Pb channel [see Figs. 2(a)–2(d)]. For the peak positions, it is noticed that our calculations describe the experimental data quite well.

We notice that in proton pick up from ^{208}Pb channel, the maxima cross sections in the reaction ^{144}Xe + ^{208}Pb are larger than those in the reaction ^{136}Xe + ^{208}Pb. The right panels of Fig. 2 show, instead, the maxima cross sections for the reaction ^{136}Xe + ^{208}Pb are much larger. The same behavior has been mentioned in Ref. [40]. Furthermore, in Figs. 2(a)–2(d) it can be seen that the advantage of the projectile ^{144}Xe with larger neutron excess induced reaction for production cross sections of neutron-rich nuclei gets more obvious with increasing number of picked up protons from the target ^{208}Pb. The above behaviors can be explained as follows. In comparison to the stable beam ^{136}Xe, due to much larger neutron excess of the projectile ^{144}Xe, the target nuclei ^{208}Pb tends to lose charge while gaining neutrons. The reason for this lies in characteristics of reaction Q values which one can visualize. In deep inelastic reactions, the role of N/Z ratio equilibration trend influences the transfer process. For the radioactive projectile ^{144}Xe, the N/Z ratio is 1.67, which is much larger than 1.54 of ^{208}Pb. However, the N/Z ratio of ^{136}Xe is smaller than that of ^{208}Pb. On the other side, this can also explain the phenomenon that for production of transtarget nuclei, the cross sections are strongly suppressed in the reaction ^{144}Xe + ^{208}Pb, although the radioactive projectile ^{144}Xe still shows advantages for production cross sections of very neutron-rich transtarget nuclei, in comparison with ^{136}Xe. Therefore, it can be concluded that radioactive beam ^{144}Xe is more favorable to produce neutron-rich nuclei in proton pick up from targets channel rather than produce transtarget nuclei.

In Fig. 3, we show the yield distributions of fragments as a function of their N/Z ratios in the transfer reaction ^{132}Sn + ^{208}Pb at $E_{\rm c.m.} = 4$, 5, 6, 7, and 8 MeV/nucleon. Yields for different incident angular momentums are summed with weights of geo-

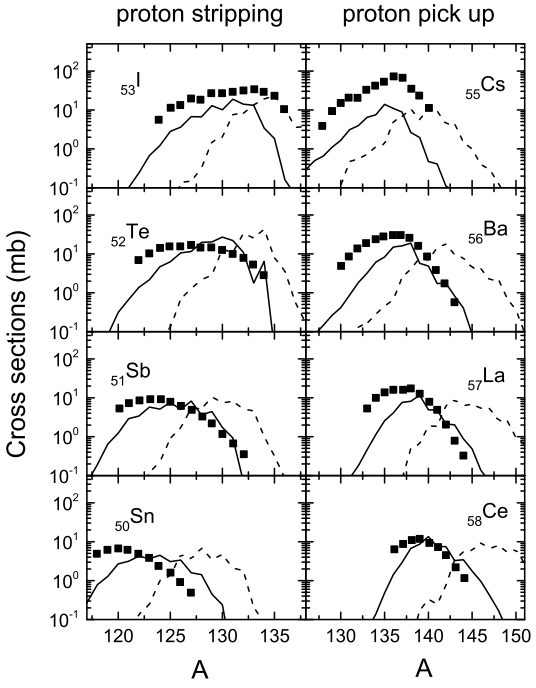

Fig. 1. Comparison of calculated production cross sections for the various projectile-like fragments (PLFs) in the reaction ^{136}Xe + ^{198}Pt with the experimental data [14]. The solid and dashed lines are distributions of final and primary fragments, respectively. The incident energy $E_{\rm c.m.} = 643$ MeV.

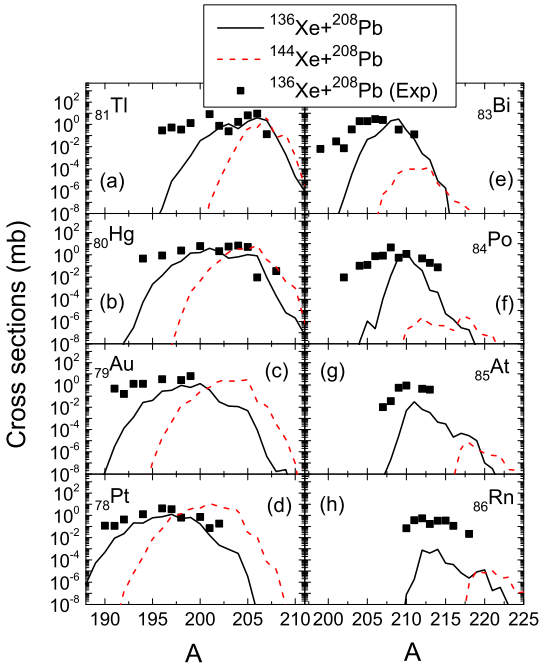

Fig. 2. (Color online.) Comparison of calculated cross sections for synthesizing various TLFs in transfer reactions ^{136}Xe + ^{208}Pb with experimental data [13] at $E_{\rm c.m.} = 450$ MeV $= 1.06 \times V_{\rm CN}$. $V_{\rm CN}$ is the interaction potential at the touching point (tip-tip). The calculated cross sections in collisions of ^{208}Pb with much larger neutron excess projectile ^{144}Xe are also shown. The incident energy equals 1.06 times corresponding $V_{\rm CN}$.

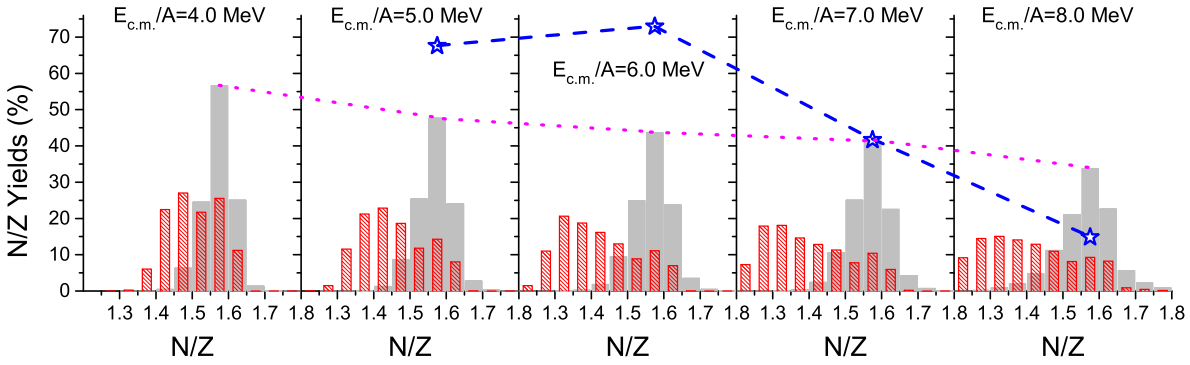

Fig. 3. (Color online.) Yield distributions of fragments as a function of their N/Z ratios for five different incident energies in the transfer reaction ^{132}Sn + ^{208}Pb. The N/Z ratio is discretized by 0.05. The light gray columns and columns with dense pattern denote the yields of primary and final fragments, respectively. The N/Z ratios for ^{132}Sn and ^{208}Pb are 1.64 and 1.54, respectively. Columns showing the yields of the primary fragments with charge equilibrium to the value $N/Z = 1.58$ at different incident energies are connected with dotted line. The stars, which connected with dashed line, denote the yields of fragments with charge equilibrium to the value $N/Z = 1.58$ calculated within TDHF theory [24].

metric cross sections. In our work, it is shown that the yield of charge-equilibrated primary fragments is highest for each incident energy. With the increasing incident energy the yield of charge-equilibrated primary fragments decreases gradually and the distribution gets wider, which are mainly due to increasing yields of exotic fragments. The DNS model can describe the production probability of all possible fragments, including very exotic ones with very low yields. Therefore, the evolution of yield distribution with the increasing incident energy is continuous. However, in Ref. [24], within the framework of TDHF, the authors pointed out that there was an upper limit of the bombarding energy for the fast and significant charge equilibration. In Fig. 3, the stars connected with dashed line are results get from Ref. [24], which denote the yields of fragments with charge equilibrium to the value N/Z =1.58 at $E_{\mathrm{c.m.}} = 5$, 6, 7, and 8 MeV/nucleon. It can be seen that with the increasing incident energy the yield of charge-equilibrated fragments is almost constant at the beginning, and a clear decrease is noticed for $E_{\mathrm{c.m.}}/A \geq 7$ MeV. The charge-equilibration dynamics is more prominent in the TDHF model. The influences of contacting time and individual single particle motion on charge equilibration can explain the behavior of the TDHF results as shown in Ref. [24]. In order for the fast charge equilibration to occur, the relative velocity of the two nuclei at the collision must be below the velocities corresponding to the proton or neutron Fermi momenta of both nuclei.

Fig. 3 also shows the yield distributions of final fragments. We notice that the yields of final fragments in low N/Z region get more prominent with increasing incident energy. This is mainly because the primary fragments evaporate more neutrons for the reaction system with higher incident energy. Therefore, the incident energies are usually taken as 1.05–1.1 times larger than Coulomb barrier for production of neutron-rich nuclei.

Fig. 4 shows the calculated cross sections for the production of the final reaction products with $Z = 72$–77 in damped collisions of ^{136}Xe, ^{139}Xe, ^{144}Xe, and ^{132}Sn projectiles with ^{208}Pb target. The collision energies were adjusted in such a way that for all cases they are 1.1 times the corresponding potential energies of contact (tip-to-tip) configurations of colliding nuclei. It can be seen that radioactive beams enhance the production cross sections of neutron rich nuclei. As can be seen the curves are shifted to higher mass number region with increasing atomic number of surviving heavy nuclei. In our calculation, it is noticed that many unknown neutron-rich nuclei can be produced with cross section of > 0.1 μb in radioactive induced transfer reactions and the production cross sections of unknown neutron-rich nuclei in the reaction ^{144}Xe + ^{208}Pb are at least two orders of magnitude larger than those in the reaction ^{136}Xe + ^{208}Pb.

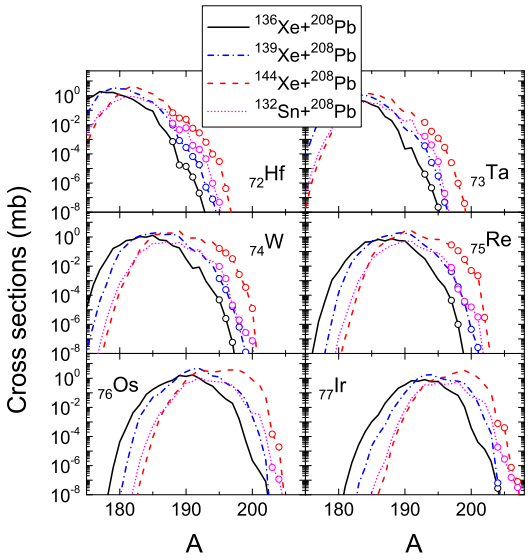

Fig. 4. (Color online.) Cross sections for producing isotopes of the elements with $Z = 72$–77 in the transfer reactions ^{136}Xe + ^{208}Pb (solid lines), ^{139}Xe + ^{208}Pb (dash-dotted lines), ^{144}Xe + ^{208}Pb (dashed lines) and ^{132}Sn + ^{208}Pb (dotted lines). The incident energy $E_{\mathrm{c.m.}} = 1.1 \times V_{\mathrm{CN}}$. The circles denote the unknown neutron-rich isotopes.

We extract the production cross sections of nuclei with neutron closed shell $N = 126$ from Fig. 4 and show them in Fig. 5. A strong enhancement of production cross sections can be seen for nuclei with $Z < 82$ in radioactive beam induced transfer reactions. The open symbols denote the unknown nuclei. One can see that the cross sections of producing unknown nuclei in the reaction ^{144}Xe + ^{208}Pb are several orders of magnitude higher than those in the reaction ^{136}Xe + ^{208}Pb. The nuclei ^{201}Re, ^{200}W, and ^{199}Ta can be produced with quite high cross sections through the reaction ^{144}Xe + ^{208}Pb. As we known, for the choice of optimal combinations, the beam intensities should be considered.

It is clearly that the production rate governs the choice of reactions. We show the values of "cross section×beam intensity" factor ($\sigma \times \phi$) for the deep inelastic collisions of stable beam ^{136}Xe and radioactive beams ^{139,144}Xe with ^{208}Pb target for producing nuclei ^{203}Ir$_{126}$, ^{202}Os$_{126}$, ^{201}Re$_{126}$, and ^{200}W$_{126}$ in Fig. 6. The incident energy $E_{\mathrm{c.m.}} = 1.1 \times V_{\mathrm{CN}}$. The estimated beam intensities proposed in SPIRAL2 project for ^{139}Xe and ^{144}Xe are taken from Ref. [35]. The

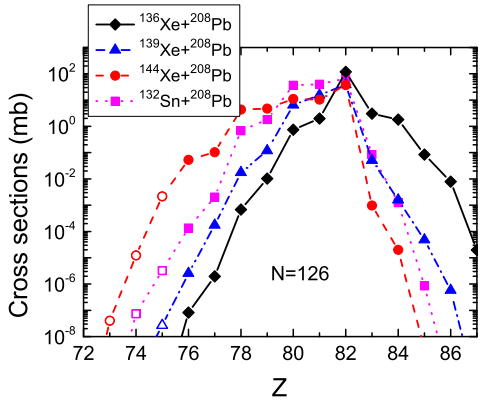

Fig. 5. (Color online.) Yields of nuclei with neutron closed shell $N = 126$ in collisions of ^{136}Xe, ^{139}Xe, ^{144}Xe, and ^{132}Sn with ^{208}Pb. The incident energy $E_{\mathrm{c.m.}} = 1.1 \times V_{\mathrm{CN}}$. Open symbols denote unknown isotopes. The lines are used to guide the eye.

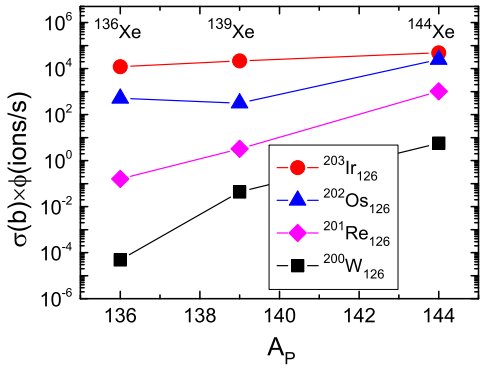

Fig. 6. (Color online.) "Cross section×beam intensity" factor ($\sigma \times \phi$) in collisions of ^{136}Xe, ^{139}Xe, and ^{144}Xe projectiles and ^{208}Pb target for production of nuclei ^{203}Ir$_{126}$, ^{202}Os$_{126}$, ^{201}Re$_{126}$, and ^{200}W$_{126}$. The radioactive beam intensities are proposed in SPIRAL2 [35]. The lines are used to guide the eye.

beam intensity of $> 10^8$ ions/s for ^{144}Xe is noticed. The intensity of the stable beam ^{136}Xe is taken as 6.2×10^{12} ions/s [41]. It is found that the radioactive beams show advantages for producing unknown neutron-rich nuclei around the $N = 126$ shell closure, in comparison with the stable beam ^{136}Xe. Further more, it is noticed that the advantages of radioactive beams get more obvious for producing nuclei with less charge number. This is mainly due to the more obvious advantages of production cross sections for producing neutron-richer nuclei in large neutron excess projectile induced reactions, as described in Figs. 2(a)–2(d).

4. Summary

Within the framework of the DNS model, the transfer reactions ^{136}Xe + ^{198}Pt, $^{136-144}$Xe + ^{208}Pb, and ^{132}Sn + ^{208}Pb are investigated. The influences of projectile neutron excess on production cross sections of TLFs are studied through reactions ^{136,144}Xe + ^{208}Pb. It is found that, due to N/Z ratio equilibration, the radioactive projectile ^{144}Xe with large neutron excess shows great advantages for cross sections of producing neutron-rich nuclei with charge number less than targets, and the cross sections are strongly suppressed for producing transtarget products. We conclude that it is favorable to produce neutron-rich nuclei in proton pick up from targets channel rather than produce transtarget nuclei by using radioactive beams. The evolution of yield distributions of fragments as a function of their N/Z ratios with the increasing incident energy are also investigated and compared with the TDHF model calculations. It is found that the yield of charge-equilibrated primary fragments is highest for each incident energy and decreases gradually with the increasing incident energy.

The production cross sections of several unknown neutron-rich nuclei with $Z = 72$–77 are predicted in the reactions $^{136-144}$Xe + ^{208}Pb and ^{132}Sn + ^{208}Pb. We notice that several unknown neutron-rich nuclei can be produced with quite large cross sections (> 0.1 μb) in radioactive beam induced transfer reactions. The production cross sections of unknown neutron-rich nuclei in the reaction ^{144}Xe + ^{208}Pb are at least two orders of magnitude larger than those in the reaction ^{136}Xe + ^{208}Pb. Further more, the radioactive projectiles ^{139,144}Xe in collisions of the target ^{208}Pb, considering beam intensities as well, for production of neutron-rich nuclei around the $N = 126$ shell closure are investigated for the first time. It is found that, based on the beam intensities proposed in SPIRAL2 project, radioactive beams show great advantages for producing neutron-rich nuclei with $N = 126$ in comparison to the stable beam ^{136}Xe. We also find that the advantages of radioactive beams get more obvious for producing neutron-richer nuclei with $N = 126$. In the future, with the development of the modern radioactive beam facilities, radioactive beam induced transfer reactions will be promising approaches to fill the blank of nuclear map around last r-process "waiting point".

Acknowledgements

This work was supported by the Natural Science Foundation of Guangdong Province, China (Grant No. 2016A030310208); the National Natural Science Foundation of China under Grants No. 11605296, No. 11405278, No. 11505150, and No. 11635003; the Fundamental Research Funds for the Central Universities under Grant No. 15lgpy30; and the China Postdoctoral Science Foundation under Grant No. 2015M582730.

References

[1] K.D. Hildenbrand, H. Freiesleben, F. Pühlhofer, W.F.W. Schneider, R. Bock, D.V. Harrach, H.J. Specht, Phys. Rev. Lett. 39 (1977) 1065.
[2] M. Schädel, et al., Phys. Rev. Lett. 41 (1978) 469.
[3] H. Freiesleben, K.D. Hildenbrand, F. Pühlhofer, W.F.W. Schneider, R. Bock, D.V. Harrach, H.J. Specht, Z. Phys. A 292 (1979) 171.
[4] M. Schädel, et al., Phys. Rev. Lett. 48 (1982) 852.
[5] K.J. Moody, et al., Phys. Rev. C 33 (1986) 1315.
[6] R.B. Welch, et al., Phys. Rev. C 35 (1987) 204.
[7] D.C. Rafferty, M. Dasgupta, et al., Phys. Rev. C 94 (2016) 024607.
[8] W. Loveland, A.M. Vinodkumar, D. Peterson, J.P. Greene, Phys. Rev. C 83 (2011) 044610.
[9] A. Vogt, et al., Phys. Rev. C 92 (2015) 024619.
[10] M.V. Pajtler, S. Szilner, et al., Nucl. Phys. A 941 (2015) 273.
[11] W. Królas, R. Broda, et al., Nucl. Phys. A 832 (2010) 170.
[12] E.M. Kozulin, et al., Phys. Rev. C 86 (2012) 044611.
[13] J.S. Barrett, W. Loveland, et al., Phys. Rev. C 91 (2015) 064615.
[14] Y.X. Watanabe, Y.H. Kim, et al., Phys. Rev. Lett. 115 (2015) 172503.
[15] V.I. Zagrebaev, W. Greiner, Phys. Rev. C 83 (2011) 044618.
[16] V. Zagrebaev, W. Greiner, Phys. Rev. Lett. 101 (2008) 122701.
[17] W. Mayer, et al., Phys. Lett. B 152 (1985) 162.
[18] V.I. Zagrebaev, W. Greiner, J. Phys. G, Nucl. Part. Phys. 34 (2007) 2265.
[19] V.I. Zagrebaev, W. Greiner, Phys. Rev. C 87 (2013) 034608.
[20] C. Golabek, C. Simenel, Phys. Rev. Lett. 103 (2009) 042701.
[21] D.J. Kedziora, C. Simenel, Phys. Rev. C 81 (2010) 044613.
[22] K. Sekizawa, K. Yabana, Phys. Rev. C 88 (2013) 014614.
[23] K. Sekizawa, K. Yabana, Phys. Rev. C 93 (2016) 054616.
[24] Y. Iwata, T. Otsuka, J.A. Maruhn, N. Itagaki, Phys. Rev. Lett. 104 (2010) 252501.
[25] N. Wang, L. Guo, Phys. Lett. B 760 (2016) 236.
[26] K. Zhao, Z. Li, Y. Zhang, N. Wang, Q. Li, C. Shen, Y. Wang, X. Wu, Phys. Rev. C 94 (2016) 024601.
[27] C. Li, F. Zhang, J. Li, L. Zhu, J. Tian, N. Wang, F.S. Zhang, Phys. Rev. C 93 (2016) 014618.
[28] R. Yanez, W. Loveland, Phys. Rev. C 91 (2015) 044608.
[29] G.G. Adamian, N.V. Antonenko, D. Lacroix, Phys. Rev. C 82 (2010) 064611.
[30] L. Zhu, Z.Q. Feng, F.S. Zhang, J. Phys. G, Nucl. Part. Phys. 42 (2015) 085102.

[31] G.G. Adamian, N.V. Antonenko, V.V. Sargsyan, W. Scheid, Phys. Rev. C 81 (2010) 024604.
[32] L. Zhu, J. Su, W.J. Xie, F.S. Zhang, Phys. Rev. C 94 (2016) 054606.
[33] Z.Q. Feng, G.M. Jin, J.Q. Li, Phys. Rev. C 80 (2009) 067601.
[34] Yu.E. Penionzhkevich, G.G. Adamian, N.V. Antonenko, Phys. Lett. B 621 (2005) 119.
[35] S. Gales, Prog. Part. Nucl. Phys. 59 (2007) 22.
[36] G.G. Adamian, N.V. Antonenko, W. Scheid, Phys. Rev. C 68 (2003) 034601.
[37] P. Möller, J.R. Nix, W.D. Myers, W.J. Swiatecki, At. Data Nucl. Data Tables 59 (1995) 185.
[38] L. Zhu, J. Su, F.S. Zhang, Phys. Rev. C 93 (2016) 064610.
[39] J.Q. Li, G. Wolschin, Phys. Rev. C 27 (1983) 590.
[40] C.H. Dasso, G. Pollarolo, A. Winther, Phys. Rev. Lett. 73 (1994) 1097.
[41] W. Loveland, Phys. Rev. C 76 (2007) 014612.